AMERICAN JOURNAL OF PHYSIOLOGY
ENDOCRINOLOGY AND METABOLISM.

Am J Physiol Endocrinol Metab 328: E289–E296, 2025.
First published January 24, 2025; doi:10.1152/ajpendo.00459.2024

METHODS AND RESOURCES

Quantitative interpretation and modeling of continuous nonprotein respiratory quotients

Zhuohui Gan,[1]* Christian J. M. I. Klein,[1,2]* Jaap Keijer,[1] and Evert M. van Schothorst[1]

[1]*Human and Animal Physiology, Wageningen University, Wageningen, The Netherlands and* [2]*TSE Systems GmbH, Berlin, Germany*

Abstract

The respiratory exchange ratio (RER), which is the ratio of total carbon dioxide produced over total oxygen consumed, serves as a qualitative measure to determine the substrate usage of a particular organism on the whole body level. Quantification of RER by its direct conversion into %glucose- (%G_{ox}) and %lipid oxidation (%L_{ox}) at a given timepoint can be done by utilizing nonprotein respiratory quotient tables. These tables, however, are limited to specific increments, and intermediate RER values are not covered by these tables. RER data are mostly continuous, which requires faithful interpolation, which we aimed for here. We first determined, statistically and schematically, that linear interpolation would lead to incorrect values. Therefore, we constructed a new mathematical model as an interpolating strategy to translate continuous RER values into correct values of %G_{ox} and %L_{ox}. We validated our new mathematical model against the original table by Péronnet and Massicotte (*Can J Sport Sci* 16: 23–29, 1991), against a linear interpolation of these data, as well as against a model based on an exponential approach using a dataset of a nutritional intervention study in mice. This showed that our model outperforms the other methods, providing more accurate data. We conclude that applying our mathematical model will lead to an increase in data quality and offer a very simple, straightforward approach to obtain the best %G_{ox} and %L_{ox} levels from continuous RER values.

NEW & NOTEWORTHY With the here proposed mathematical model, we provide a new tool to convert continuous RER data into more accurate estimations of %G_{ox} and %L_{ox}. It circumvents the use of nonprotein respiratory quotient tables and thereby aids and simplifies by automating the conversions. The model can further be implemented into software commonly used for indirect calorimetry measurements and thereby provides %G_{ox} and %L_{ox} data in real-time during a running experiment.

carbohydrate metabolism; energy metabolism; indirect calorimetry; lipid metabolism; oxygen consumption

INTRODUCTION

In physiology and metabolism, indirect calorimetry (InCa) is the gold standard method to measure oxygen consumption and carbon dioxide production, from which energy expenditure (EE) and substrate usage at the whole body level, represented by the respiratory exchange ratio (RER), are calculated (1–3). At the cellular level, RER is referred to as the respiratory quotient (RQ), which lacks for instance the acid-base bicarbonate balance of blood, and it is also defined by the ratio of carbon dioxide production over oxygen consumption. Although in the past, the term RQ was commonly used, we will hereafter refer to RER since it reflects the whole body level measured by InCa. In preclinical mouse studies, InCa measurements provide valuable insights into metabolism under different situations [e.g., fed vs. fasted (4), different diets (5) or pharmacological interventions (6), different physical activity (7), life stages (8), the strain of mice (9) or differences in environmental factors, including low-oxygen challenges (8) or cold challenges (10), etc.]. Standard InCa measurements are part of the Mouse Phenotyping Consortium project to characterize the animals in detail (11).

To obtain detailed insights, RER values can be utilized to estimate the percentage of EE (%EE) derived both from carbohydrates, that is, glucose oxidation (%G_{ox}), and from lipids, that is, lipid oxidation (%L_{ox}). Since the accurate measurement of protein oxidation on the whole body level is very challenging, protein oxidation is commonly neglected and the RER is referred to as nonprotein (NP)-RER, which thus reflects the sum of %G_{ox} and %L_{ox} being always 100%. Relative G_{ox} and L_{ox} can further be used to quantify total (endogenous and exogenous) substrate oxidation (either fat or carbohydrate) taking the energy equivalent of the specific substrate into account (12). RER values above 1 are either indicative of lipogenesis originating from glucose conversions by intermediary metabolism, on top of full %G_{ox} (13, 14), or of increased circulating lactate levels, for example, following high-intensity exercise, and consequential blood acid-base balance increased carbon dioxide release (15, 16), and will both further not be considered.

*Z. Gan and C. J. M. I. Klein contributed equally to this work.
Correspondence: E. M. van Schothorst (evert.vanschothorst@wur.nl).
Submitted 14 November 2024 / Revised 3 December 2024 / Accepted 9 January 2025

The table by Péronnet and Massicotte is based on and extends the pivotal work of Lusk (17, 18). It is currently and ubiquitously being used for the conversion of RER into $\%G_{ox}$ and $\%L_{ox}$ for the range of 0.7036 (100% L_{ox}) until 0.996 (100% G_{ox}) (12). However, the table uses 0.005 incremental data points of RER ranging from 0.705 to 0.995, which prohibits usage for the continuous variable RER in these conversions. These continuous RER values are nowadays commonly generated by modern and state-of-the-art InCa systems thanks to improvements in sensor resolution and accuracy, and a continuous conversion model or formula is therefore needed. One way to interpolate the data between the 0.005 incremental points is to apply a linear approach assuming a linear relationship between RER and $\%G_{ox}$ or $\%L_{ox}$. Such an approach would provide a simple, easy, and quick mathematical step and could lead to immediately available $\%G_{ox}$ and $\%L_{ox}$ values per measured RER.

Here, we first tested the linear relationship between RER and $\%G_{ox}$. The observed nonlinearity stressed the need for an improved interpolation method. Therefore, we here constructed a new mathematical model to estimate $\%G_{ox}$ and $\%L_{ox}$ at the highest accuracy level, enabling the utilization of continuous NP-RER data points for continuous $\%G_{ox}$ and $\%L_{ox}$ values and tested this against other methods.

METHODS AND RESULTS

The Relationship between RER and Oxygen Consumption by Carbohydrate Oxidation Is Nonlinear

The relationship between RER and relative energy production from glucose oxidation ($\%G_{ox}$) looks linear based on data from Table 2 in the publication by Péronnet and Massicotte (12). To test this, we constructed a linear equation with the full range of these data (0.7036–0.996):

$$y = 341.63x - 239.26, \tag{1}$$

where x and y stand for RER and $\%G_{ox}$, respectively.

As the sum of $\%G_{ox}$ and $\%L_{ox}$ equals 100% at each RER value, we selected the $\%G_{ox}$ to be variable for the model, but $\%L_{ox}$ can easily be calculated from it. The parameters were optimized using the lsqcurvefit function from the optimization toolbox of MATLAB (MATLAB v. R2022a, MathWorks Inc., Natick, MA). Although the coefficient of determination (R^2) of this fitting is as high as 99.9%, we noticed that the RER-$\%G_{ox}$ relationship is not strictly linear (Supplemental Fig. S1). Therefore, a linear model might not be the best fit to interpolate the RER and $\%G_{ox}$ data of Péronnet and Massicotte's table.

To prove the nonlinearity of the relationship between RER and $\%G_{ox}$, we established a linear equation using the second (RER = 0.705) and the second to last (RER = 0.995) data points from Péronnet and Massicotte's Table 2, as the first (RER = 0.7036) and last (RER = 0.996) data points do not follow the increment steps (0.005) of the remaining RER data points (see Supplemental Fig. S1 for comparison). The linear equation (*Eq. 2*) thus obtained is:

$$y = 341.72x - 240.42, \tag{2}$$

where x and y stand for RER (range 0.705–0.995) and $\%G_{ox}$, respectively.

If there was a strict linear relationship between RER and $\%G_{ox}$ in Péronnet and Massicotte's data using our *Eq. 2*, the $\%G_{ox}$ values of both approaches would ideally be the same for each individual RER. In other words, the delta values ($\%G_{ox}$) between both approaches would be zero (strictly linear) or at least very small. However, Fig. 1*A* clearly indicates that for each individual RER value, $\%G_{ox}$ from the original table is larger than the value generated by the simple linear equation (*Eq. 2*). This is especially striking for the RER values in the middle area, representing the range where most RER values are measured during a standard 24-h timespan. The differences are distributed as an arc-like shape (Fig. 1*A*, dashed line), showing the nonlinear relationship between RER and $\%G_{ox}$ in Péronnet and Massicotte's table. Figure 1*B* schematically emphasizes such an arc-like nonlinear curve. The curvature of the RER-$\%G_{ox}$ curve is rather quite small relative to 100% G_{ox}, representing at most 1.7%G_{ox} at RER = 0.825 (Fig. 1*A*; see Supplemental Table S1 for raw data).

To find a better-fitting and more accurate model, we next concentrated on assessing the curvature. Since the incremental steps of the RER values remain constant (0.005, except for the first and last data point), examining the magnitude of changes in delta $\%G_{ox}$ would provide us greater

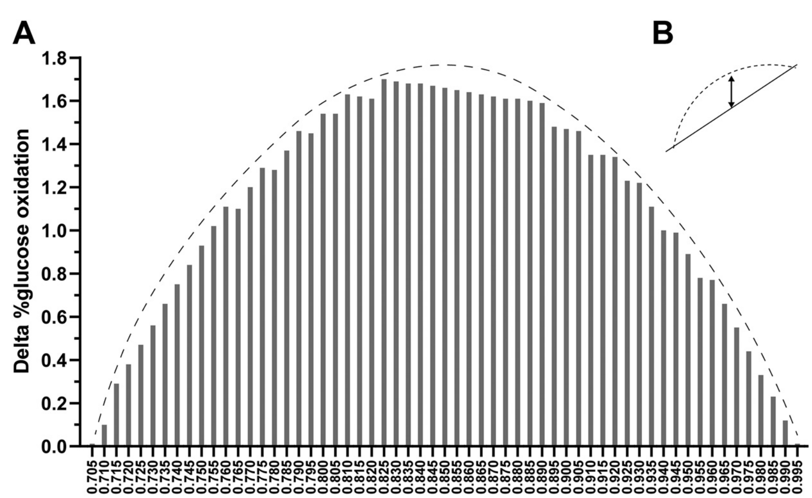

Figure 1. The differences in $\%G_{ox}$ derived from RER between Péronnet's data and values generated by a linear equation. *A*: the distribution of $\%G_{ox}$ differences (delta) between Péronnet and Massicotte's data and values generated by *Eq. 2*. The *x*-axis presents RER and the *y*-axis presents the delta percentage of energy from glucose oxidation ($\%G_{ox}$) between the two approaches (bars) and its arc-like distribution (dashed line). *B*: a schematic presentation of the $\%G_{ox}$ (ordinate) from Péronnet and Massicotte's data (arc, dashed line) vs. $\%G_{ox}$ values generated by linear *Eq. 2* (straight line) and their differences (area between the lines, indicated by the arrow-headed line) for RER values 0.705 till 0.995 (abscissa). RER, respiratory exchange ratio.

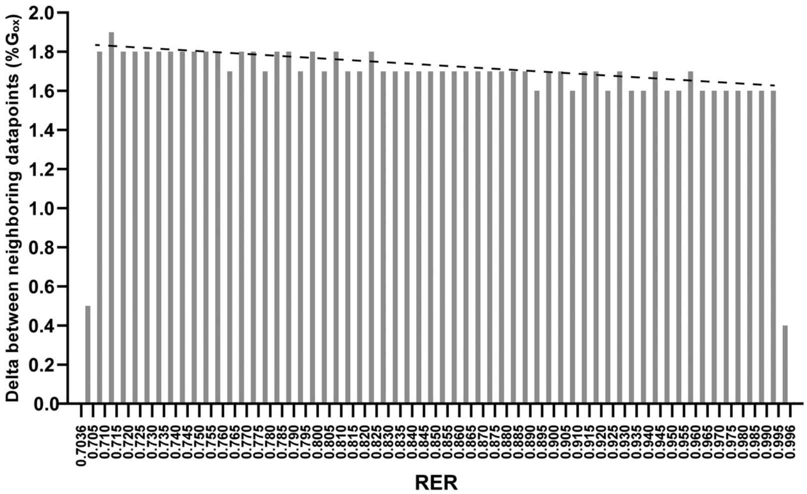

Figure 2. The step differences in %G_{ox} between two neighboring RER datapoints in Péronnet and Massicotte's Table 2. The *x*-axis presents RER values and the *y*-axis presents the delta percentage of energy from glucose oxidation (%G_{ox}) of two neighboring RER values. The step length is according to incremental steps in Table 2 by Péronnet and Massicotte (1). Dashed line: a schematic presentation of the tendency of step differences. RER, respiratory exchange ratio.

insights into the properties of the curvature. Therefore, we calculated the step differences, which are the differences between two neighboring data points to estimate its curvature (Fig. 2; see Supplemental Table S1 for raw data). The step differences are in the range of 1.6%G_{ox}–1.9%G_{ox}, except for the first (RER = 0.7036) and last (RER = 0.996) RER value and show a very mild decline represented by the dashed line (Fig. 2). Further considering that the values of step differences were only 1%–5% of corresponding Péronnet and Massicotte's data (data not shown), this decline is as mild as a near-steady state but not neglectable. Therefore, we aimed to find an alternative and better-fitting model.

The Modified Michaelis–Menten Model Is the Best Fit to Interpret Péronnet and Massicotte's Data Quantitatively

There are distinct types of models to simulate a near-steady state with a small curvature. An exponential equation with a negative exponent is the most common model to simulate a near-steady state. By fitting Péronnet and Massicotte's data to such an exponential equation, we got *Eq. 3*:

$$y = 674.17 - 991.69 \times e^{-0.5482x}, \tag{3}$$

where x and y stand for RER and %G_{ox}, respectively.

To evaluate the goodness of fit of each alternative model, we calculated the total residual and normalized squared standard derivation (SSD). The total residual is calculated by $\sum_1^n (y_i - x_i)^2$, where y_i is the value generated by the model, x_i is the data from Péronnet and Massicotte's table, and n is the total number of RER data points in their table. SSD is calculated by $\sqrt{\frac{\sum_1^n (y_i - x_i)^2}{n}}$, which is better to compare fitting results with different numbers of input data. The exponential model (*Eq. 3*) indicates a significant improvement compared with the linear model (*Eq. 1*), shown by the much smaller total residual at 0.695 versus 17.875 and SSD at 0.107 versus 0.541 (Table 1).

A Michaelis–Menten equation, which is widely used in the field of quantitative physiology, can also simulate a near-steady state. Based on the feature of Péronnet and Massicotte's data, we modified the general Michaelis–Menten (MM) equation as $y = \frac{A(x-B)}{x+C}$, where A, B, and C are parameters that needed to be determined. We define A as the capacity, B as the origin, and C as the C_{50} value of the modified MM (mMM) equation. Using the optimization toolbox function lsqcurvefit of MATLAB, we determined these parameters and established the following equation for %G_{ox} (*Eq. 4*):

$$y = \frac{1530.7 \times (x - 0.7036)}{3.4825 + x} \tag{4}$$

with x representing the RER value and y the corresponding %G_{ox}.

As the sum of %G_{ox} and %L_{ox} are defined as 100%, the corresponding formula for %L_{ox} is thus *Eq. 5*:

$$y = 100 - \frac{1530.7 \times (x - 0.7036)}{3.4825 + x} = \frac{1430.7 \times (0.9962 - x)}{3.4825 + x} \tag{5}$$

with x representing the RER value and y the corresponding %L_{ox}.

The mMM equation simulates Péronnet and Massicotte's data exceptionally well with a total residual as small as 0.048 for 61 data points, which are found in the %G_{ox} range of 0%–100% (Table 1). The mMM model outperforms the other models by means of total residual and SDD and therefore presents Péronnet and Massicotte's data best (Table 1, Supplemental Table S1). When we express the differences between the original table and our new mMM model graphically (similarly to Fig. 1 for the linear approach), we see that

Table 1. *A comparison of models for conversion of RER data into %G_{ox}*

Model Type	Equation	Total Residual	SSD
Linear	*Eq. 1*: $y = 341.63x - 239.26$	17.875	0.541
Exponential	*Eq. 3*: $y = 674.17 - 991.69 \times e^{-0.5482x}$	0.695	0.107
mMM	*Eq. 4*: $y = \frac{1530.7 \times (x-0.7036)}{3.4825+x}$	0.048	0.028

In the equations, x stands for RER and y stands for %G_{ox}. All equations are based on Péronnet and Massicotte's data (Table 2). G_{ox}, glucose oxidation; mMM, modified Michaelis–Menten; RER, respiratory exchange ratio; SSD, normalized squared standard derivation.

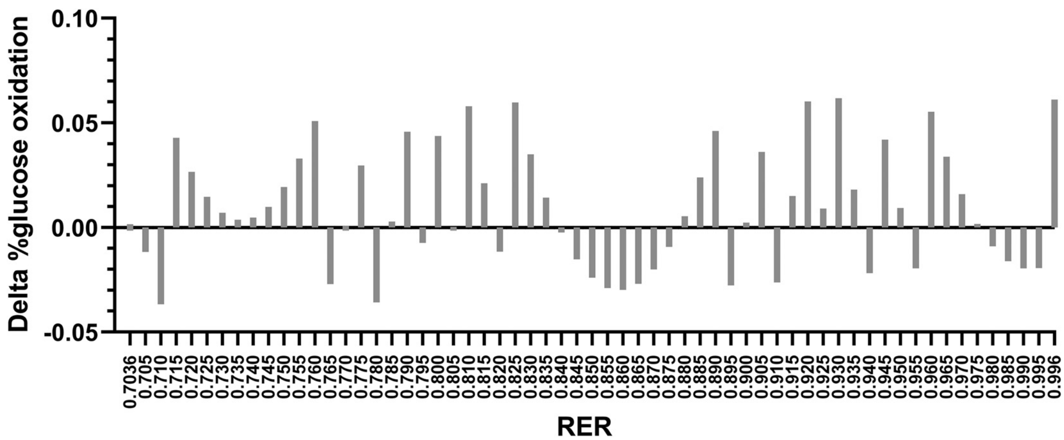

Figure 3. The differences in $\%G_{ox}$ derived from RER between Péronnet and Massicotte's data and values generated by the new mMM model. The distribution of $\%G_{ox}$ differences (delta) between Péronnet and Massicotte's data and values generated by *Eq. 4* (mMM model). The *x*-axis presents RER and the *y*-axis presents the delta of energy from glucose oxidation ($\%G_{ox}$) between the two approaches. The step length is according to incremental steps in Table 2 by Péronnet and Massicotte (1). Note the difference in delta $\%G_{ox}$ in Fig. 1 (0%–1.7%) and here (−0.04% to 0.06%). mMM, modified Michaelis–Menten; RER, respiratory exchange ratio.

the delta values are impressively small indicating an almost perfect fit (Fig. 3). Compared with a linear approach in which the largest delta value was $1.7\%G_{ox}$ (Fig. 1), with our new mMM model, all delta values are substantially smaller, with the largest delta value being just $0.06\%G_{ox}$ (Supplemental Fig. S2 for a direct graphical comparison). This represents an almost 30-fold increase in data quality compared with a linear approach. The comparison between the different models of Péronnet and Massicotte's data and the modeling fitting results are presented in Table 1, whereas Fig. 4 highlights Péronnet and Massicotte's data and the new mMM model.

The Modified Michaelis–Menten Model Is Stable and Tolerant to Variances in Input Data

A key feature of the mMM model is that this model goes exactly through the start point of Péronnet and Massicotte's table, where RER = 0.7036 and $\%G_{ox} = 0\%$ (so 100% L_{ox}). The start and last points of Péronnet and Massicotte's table are visibly out of the linear range and hence can be utilized to define the model parameters even more precisely. To validate the goodness of fit of Eqs. *4 and 5* including the first and last RER point of Péronnet's Table 2, we estimated the model parameters using first the dataset excluding the first and last data points. The results indicate that the model is quite tolerant (Table 2). For example, if the first point was excluded from the parameter estimation, RER = 0.7036 still represents $\%G_{ox} = 0.00\%$. To further evaluate the model tolerance, a model fitting was applied using different numbers of data from Péronnet and Massicotte's table. The results indicate that the mMM model is highly tolerant to variance in input data, and only with the loss of key data (the first 10 and last 10 data points) do the parameters slightly vary

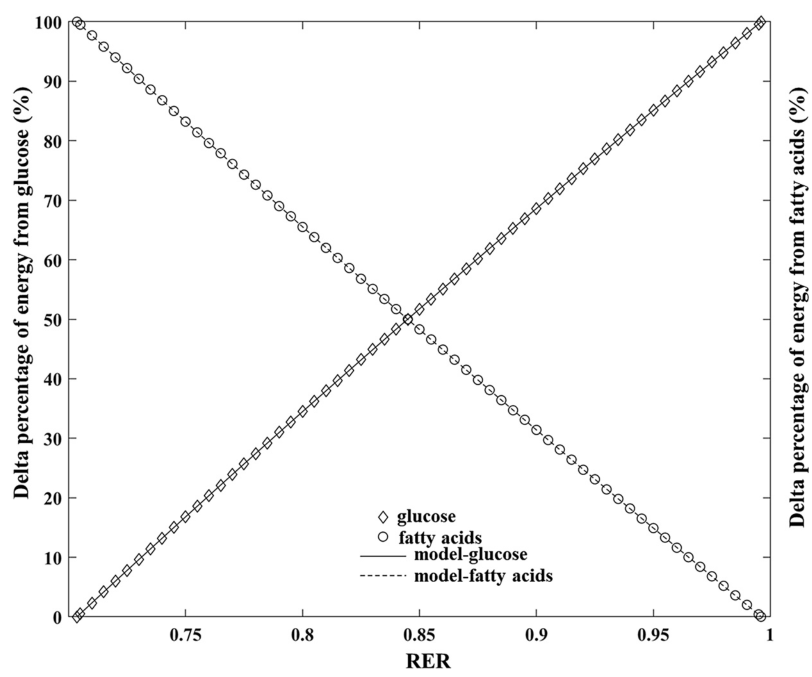

Figure 4. Original G_{ox} data derived from Péronnet and Massicotte's data (Table 2) vs. the mMM model (*Eq. 4*). The *x*-axis presents the RER values with the relative oxidation levels of glucose (*left*) and fatty acids (*right*) on the *y*-axis. Symbols (diamonds: glucose, circles: fatty acids) indicate original incremental data, whereas lines (full line: glucose, dashed line: fatty acids) indicate mMM model continuous data output. G_{ox}, glucose oxidation; mMM, modified Michaelis–Menten; RER, respiratory exchange ratio.

Table 2. *Tolerance estimation for equation fit*

Input Data	RER	*A*	*B*	*C*	SSD
All 61 data points	0.7036–0.996	1,530.7	0.7036	3.4825	0.0281
Data points 2–60	0.705–0.995	1,530.7	0.7036	3.4825	0.0277
1 of every 3 data points	0.7036–0.995	1,531.3	0.7036	3.4850	0.0277
Data points 1–20 and 42–61	0.7036–0.795, 0.905–0.996	1,517.0	0.7036	3.4421	0.0271
Data points 11–51	0.750–0.950	1,573.7	0.7035	3.6083	0.0284

The parameters for the mMM equation $y = \frac{A(x-B)}{x+C}$ were estimated by including different subsets of numbers of the full range of 61 RER data points taken from Péronnet and Massicotte's Table 2. First data point is RER = 0.7036, last RER = 0.996. mMM, modified Michaelis–Menten; RER, respiratory exchange ratio; SSD, normalized squared standard derivation.

(Table 2). Taking both the excellent quality of the model's fitting and the high tolerance to input data variance, we consider the mMM model as the best fit to quantitatively describe the pattern of $\%G_{ox}$ from nonprotein RER values.

The determined mMM formulae (*Eqs. 4* and *5*) optimize the RER step length (increments) from 0.005 to 0.001 and therefore allow a much more precise estimation of $\%G_{ox}$ from the nonprotein respiratory quotient. Furthermore, the mMM formula can be applied to any continual RER data point, even smaller than 0.001 increments. Therefore, it is only limited by the data output generated by the InCa system in place. As such, it can also be applied to directly, and correctly, convert RER values within the InCa software into $\%G_{ox}$ and $\%L_{ox}$ values.

Proof of Principle and Applicability

We here show that the mMM model gives mathematically and statistically the best fit for the estimation of $\%G_{ox}$ and $\%L_{ox}$ from the nonprotein respiratory quotient (RER ≤ 1). As a proof of principle and to test its applicability, we applied the different models (linear, exponential, and mMM) to a previously published dataset (19) derived from mice that were fed either a low- or a high-fat diet (LFD and HFD, respectively). Focusing here on RER specifically, both the 24 h and its subdivision in light and dark phase periods were analyzed (Table 3).

On an LFD, calculated $\%G_{ox}$ is highly comparable between the different approaches as represented by the delta values for mean 24 h (0.01, 0.01, and 0.01 for linear, exponential, and mMM model, respectively), mean during the light phase (LP; 0.08, 0.03, and 0.04), and mean during the dark phase (DP; 0.07, 0.01, and 0.02), respectively. On an HFD, however, only $\%G_{ox}$ calculated by the mMM model is very similar to the original approach and outperforms the linear and exponential models, as is indicated by the delta values for 24 h (0.36, 0.09, and 0.01), LP (0.39, 0.09, and 0.00), and DP (0.32, 0.09, and 0.01), respectively (Table 3).

DISCUSSION

During indirect calorimetry measurements, the ratio of CO_2 production over O_2 consumption (RER) gives insights into the substrate usage (carbohydrates and lipids) of an organism at a particular timepoint. The ubiquitously used table of nonprotein respiratory quotient by Péronnet and Massicotte describes the percentages of energy retrieved from glucose and lipid oxidation (RER ≤ 1) with 0.005 incremental steps (12). In the current work, we follow up on their pivotal work and introduce a modified Michaelis–Menten model (mMM, *Eq. 4*) to calculate $\%G_{ox}$ and $\%L_{ox}$ more accurately. The primary advantage of our mMM model lies in its accurate representation of the values reported by Péronnet and Massicotte, enabling precise interpolation of $\%G_{ox}$ and $\%L_{ox}$ values that are not explicitly included in their original table, simultaneously allowing for easy applicability.

The mMM model outperformed the two other models (linear and exponential models) tested and showed the best fit to interpolate the RER and $\%G_{ox}$ and $\%L_{ox}$ values underpinning its strength. To test this in practice, we applied the model to real physiological data and showed that the mMM model is very accurate. As mice on HFD versus LFD usually show quite distinct RER profiles, with middle-range RER values (HFD) versus clear higher (LFD) RER values. Results showed for mice on an LFD, that is, under conditions of relatively higher glucose over lipid oxidation levels, that a linear interpolation would lead to very comparable $\%G_{ox}$ results compared with the mMM model. This confirms that the extreme values (either high or low RER) are less prone to

Table 3. *Comparison of performance of mMM model*

			% Glucose				Delta		
Group	Period	RER	Péronnet and Massicotte	Linear (*Eq. 1*)	Expo (*Eq. 3*)	mMM (*Eq. 4*)	Linear	Expo	mMM
LFD	24 h	0.979	85.90	85.90	85.90	85.89	0.01	0.01	0.01
	LP	0.963	82.00	81.92	81.97	81.96	0.08	0.03	0.04
	DP	0.995	89.88	89.95	89.89	89.90	0.07	0.01	0.02
HFD	24 h	0.875	59.78	59.43	59.88	59.79	0.36	0.09	0.01
	LP	0.871	58.28	57.88	58.37	58.28	0.39	0.09	0.00
	DP	0.879	61.32	61.00	61.41	61.33	0.32	0.09	0.01

Mice were fed a low-fat (LFD, $n = 9$) or a high-fat (HFD, $n = 9$) diet for 12 wk (19). RER was continuously measured for 24 h, and presented as mean (24 h), or subdivided into mean 12-h light (LP, inactive) and mean 12-h dark (DP, active) phase, respectively. Calculated %glucose oxidation ($\%G_{ox}$) values are derived from converting each individual RER-datapoint into $\%G_{ox}$ and subsequent 24 h, LP, and DP means by different approaches as indicated. Also, the corresponding $\%G_{ox}$ delta values are compared with the usage of Péronnet and Massicotte's table. mMM, modified Michaelis–Menten; RER, respiratory exchange ratio.

linear interpolation errors as shown in Fig. 1, despite such a method being statistically less accurate. In such a condition, linear interpolation would generate a comparable $\%G_{ox}$ compared with our new model. On the contrary, on an HFD, where RER values are mostly in the midst of the RER range, a linear model is prone to errors as shown in Fig. 1 and would overestimate $\%G_{ox}$. Especially in such situations, our new mMM model increases the data quality by a more accurate calculation of $\%G_{ox}$. Next to estimating $\%G_{ox}$ and $\%L_{ox}$ levels more accurately from RER readings, our new mMM model has further additional advantages: first, our new model can be used directly on all RER values without any precaution for incremental step sizes as used by the tables published by Péronnet and Massicotte (12). Since modern and state-of-the-art InCa systems will measure RER data with 0.001 increments or with an even higher resolution, the new mMM models give researchers a new tool to more accurately obtain $\%G_{ox}$ and $\%L_{ox}$, especially in the middle range of the RER, where the majority of RER values are measured during a standard 24-h timespan. Second, the mathematical model is not only applicable to a single species but can be used for all species under investigation by indirect calorimetry, including but not limited to insects, birds, rodents, larger animals, such as pigs, calves, or fish, but also humans using ventilated hoods or respiration rooms. Third, with our work, we also followed the suggestion by the authors Péronnet and Massicotte and constructed a mathematical model that offers a convenient formula to easily incorporate this into InCa software to directly observe $\%G_{ox}$ and $\%L_{ox}$ values. This provides real-time insights during ongoing measurements, whereas it can also be used afterward in software commonly used for the analysis of indirect calorimetry measurements, like Excel, R, or the web-based program CalR (20).

The here presented mMM model is entirely based on the work of Péronnet and Massicotte, including assumptions and limitations in their original work, which represents a potential limitation. Péronnet and Massicotte provide a table of nonprotein respiratory quotient, which neglects the contribution of protein oxidation. Although the relative contribution of protein oxidation toward overall fuel oxidation is lower compared with carbohydrate and fat oxidation, its absolute contribution is still substantial. Although the incorporation of total protein oxidation would certainly be of added value, its assessment in practice is challenging, since it relies on sophisticated techniques and skills, includes several limitations (21–23), and inappropriate values would introduce errors (24). For example, advancements in amino acid tracer techniques have enabled the investigation of whole body protein metabolism by tracking the oxidation of isotope-labeled amino acids (25, 26), typically administered intravenously or orally. These studies often require frequent blood and/or urine sampling to monitor tracer enrichment and nitrogen excretion to be able to provide detailed insights into protein oxidation kinetics. However, the choice of tracer must be carefully considered, as different tracers yield distinct metabolic insights and results can vary significantly depending on the tracer used (27). Moreover, application in mice requires profound microsurgery skills, and their availability and costs can limit their practical application. Tracer studies are also invasive, involving precise tracer administration, rigorous study protocols, and reliance on several assumptions (25, 28). Alternatively, 24-h urinary nitrogen excretion offers a less invasive and logistically simpler approach to estimate protein oxidation and can be integrated with indirect calorimetry to yield complementary insights into the contribution of proteins, fatty acids, and carbohydrates to whole body substrate utilization. However, it sacrifices the temporal resolution required to capture dynamic variations over shorter periods, which is particularly critical for accurately assessing protein oxidation due to the highly dynamic nature of protein turnover, and it can introduce errors (24). Although tracer studies are valuable for understanding the four aspects of protein metabolism, substrate utilization, the role of protein oxidation in whole body energy balance, and determining accurate protein and amino acid requirements across populations, they are rarely performed alongside indirect calorimetry due to their complexity, invasiveness, and resource requirements. It is therefore not surprising that the quantification of protein oxidation is commonly neglected during (pre)clinical experiments. Until the present obstacles (25) have been overcome by advances in the field of measuring whole body protein oxidation, relying on nonprotein RER values seems to be the maximum feasible in the majority of (pre)clinical settings. Thus, our mMM models are most suitable in physiological conditions in which protein oxidation can be considered stable, as was already the case as researchers have used the data table by Péronnet and Massicotte to convert RER into $\%G_{ox}$ and $\%L_{ox}$ since 1991. Caution is warranted for organisms in a state of growth, recovery, or exercise, which might lead to incorrect values and interpretations (12).

The mean fatty acid composition in human adipose tissue samples served as a foundation for the calculation of mean fatty acid oxidation, which might be outdated given the fact that dietary patterns and dietary behavior have changed over the last decades, shifting, for example, to plant-based foods (29, 30), which can affect the dietary intake of fatty acids to some extent (31). Diets varying in fatty acid composition have been shown to affect lipid composition in adipose tissue in several species (32). Furthermore, it has long been known that various species differ in their lipid composition of adipose tissue, with the influence of age and collection site/depths of adipose tissue as has been shown for humans (32). Therefore, it seems worth establishing whether the fatty acid profile used for the calculations by Péronnet and Massicotte still represents the average fatty acid profiles in adipose tissues today. Until experiments are conducted to update the values of Péronnet and Massicotte for carbohydrate and fat oxidation, our current model remains valid, whereas adaptation will be quite straightforward.

Limitations of the mMM Model

Péronnet and Massicotte did not consider RER values above 1, which are frequently observed in rodent studies feeding a low-fat and high-carbohydrate chow as a standard diet. In this situation, RER values above 1 indicate lipogenesis originating from glucose on top of the 100% G_{ox} used for metabolic rate. Therefore, our mMM model is limited to RER values below 1 (0.996) and does not deal with the conversion of glucose into fat. Moreover, the table by Péronnet and Massicotte associates an RER of 0.996 with $100\%G_{ox}$, which is inconsistent with stoichiometry. Oxidation of one mole of glucose requires the consumption of six moles of oxygen, resulting in the production of six moles of carbon dioxide, yielding a CO_2/O_2 ratio of 1.000 for complete oxidation. Consequently, the mMM model presents a slight deviation from this stoichiometric relationship. It is worth highlighting that also other scientists provided tables for the conversion of nonprotein RER into $\%G_{ox}$ and $\%L_{ox}$ values, namely, Elia and Livesey (14), which also offer an equation to accurately calculate $\%G_{ox}$ and $\%L_{ox}$ suited to their published RER conversion factors. The small differences between these tables versus the one by Péronnet and Massicotte are, for instance, due to differences in selected fatty acid composition in human adipose tissue, which serves as a foundation for the underlying mathematical calculations of conversion factors. To better understand the impact of the different values between the two tables, especially associating an RER of 1.000 with $100\%G_{ox}$ and thus consistent with a stoichiometric view, we estimated the parameters for our mMM model using data from Table 4 of Elia and Livesey (14) in the ranges for RER from 0.7097 till 1.00. This resulted in the following mMM equations for $\%G_{ox}$ and $\%L_{ox}$ with x presenting the RER values:

$$\%G_{ox} = \frac{1304.1 \times (x - 0.7097)}{x + 2.7861}, \tag{6}$$

$$\%L_{ox} = 100 - \frac{1304.1 \times (x - 0.7097)}{x + 2.7861} = \frac{1204.1 \times (1 - x)}{x + 2.7861}. \tag{7}$$

By simplifying the equation in that study (Eq. 38 in Ref. 14) to our mMM formulae, we got:

$$\%G_{ox} = \frac{1305.3 \times (x - 0.7097)}{x + 2.7893}. \tag{8}$$

This equation (*Eq. 8*) is almost the same as *Eq. 6* with slight differences in parameters caused by the limited data precision of Table 4 in Elia and Livesey's study. In fact, the similarity between *Eq. 6* and *Eq. 8* confirms the effectiveness of our approach.

The aim of this study was to develop a model for improved quantitative interpretation of the conversion table of Péronnet and Massicotte (12). Our mMM model is developed to best fit the data by Péronnet and Massicotte, whereas the equation and table by Elia and Livesey simultaneously offer a valid alternative way to interpret RER values in terms of $\%G_{ox}$ and $\%L_{ox}$.

Acknowledging the differences between the two tables (*Eq. 4* vs. *Eq. 6*), we find that our mMM model (*Eq. 4*) outperforms a linear and exponential interpolation when analyzed with the same data set. Consequently, we believe that the mMM model presented here along with its parameter optimization can be widely applied to similar datasets, and hence allows to generate high-precision data more easily. Ultimately, the scientific community will determine which dataset and equation will be preferred.

Early in the previous century, Lusk published in 1924 the first revision of his table of nonprotein respiratory quotient, which inspired others to follow by continuously updating and improving his work, and it is still being used by many in the field of energy metabolism. Today, a full century after Lusk's pivotal work, with the mathematical model proposed here, we like to follow in his and other's footsteps. Although the improvements in data quality with our model might be very small in some situations, we like to remind of the original remark by Lusk in 1924: "Although the error is not great, yet it is worthy to note and of record" (17).

DATA AVAILABILITY

Raw experimental data will be made available upon reasonable request by contacting the corresponding author.

SUPPLEMENTAL MATERIAL

Supplemental Figs. S1 and S2: https://doi.org/10.6084/m9.figshare.28143512.

Supplemental Table S1: https://doi.org/10.6084/m9.figshare.28143557.

GRANTS

Z.G. is supported by the Next Level Animal Sciences (NLAS) program ("Data and Models") of the Wageningen University (Wageningen, The Netherlands), for which funding was secured by J.K. together with Werner Koopman (Human and Animal Physiology, Wageningen University). C.J.M.I.K. is an ESR fellow of the INSPIRE European Training Network. INSPIRE received funding from the EU Horizon 2020 Research and Innovation program, under the Marie Skłodowska–Curie program Grant GA 858070.

DISCLOSURES

C.J.M.I.K. is employed at TSE Systems GmbH. None of the other authors has any conflicts of interest, financial or otherwise, to disclose.

AUTHOR CONTRIBUTIONS

J.K. and E.M.v.S. conceived and designed research; Z.G. and C.J.M.I.K. performed experiments; Z.G., C.J.M.I.K., and E.M.v.S. analyzed data; Z.G., C.J.M.I.K., J.K., and E.M.v.S. interpreted results of experiments; Z.G. and C.J.M.I.K. prepared figures; Z.G., C.J.M.I.K., and E.M.v.S. drafted manuscript; Z.G., C.J.M.I.K., J.K., and E.M.v.S. edited and revised manuscript; Z.G., C.J.M.I.K., J.K., and E.M.v.S. approved final version of manuscript.

REFERENCES

1. **Even PC**, **Nadkarni NA.** Indirect calorimetry in laboratory mice and rats: principles, practical considerations, interpretation and perspectives. *Am J Physiol Regul Integr Comp Physiol* 303: R459–R476, 2012 [Erratum in *Am J Physiol Regul Integr Comp Physiol* 309: R1460, 2015]. doi:10.1152/ajpregu.00137.2012.
2. **Haugen HA**, **Chan LN**, **Li F.** Indirect calorimetry: a practical guide for clinicians. *Nutr Clin Pract* 22: 377–388, 2007. doi:10.1177/0115426507022004377.
3. **Speakman JR.** Measuring energy metabolism in the mouse–theoretical, practical, and analytical considerations. *Front Physiol* 4: 34, 2013. doi:10.3389/fphys.2013.00034.
4. **Hoevenaars FP**, **Keijer J**, **Herreman L**, **Palm I**, **Hegeman MA**, **Swarts HJ**, **van Schothorst EM.** Adipose tissue metabolism and inflammation are differently affected by weight loss in obese mice due to either a high-fat diet restriction or change to a low-fat diet. *Genes Nutr* 9: 391–11, 2014. doi:10.1007/s12263-014-0391-9.
5. **Cooling J**, **Blundell J.** Differences in energy expenditure and substrate oxidation between habitual high fat and low fat consumers (phenotypes). *Int J Obes Relat Metab Disord* 22: 612–618, 1998. doi:10.1038/sj.ijo.0800635.
6. **Loeffler M**, **Klepac K**, **Baljuls A**, **Hamilton B**, **Mayer-Wrangowski S**, **Haebel P**, **Zimmermann T.** Effects of a long-acting secretin peptide

analog alone and in combination with a GLP-1R agonist in a diet-induced obesity mouse model. *Mol Metab* 74: 101765, 2023. doi:10.1016/j.molmet.2023.101765.
7. **O'Neal TJ**, **Friend DM**, **Guo J**, **Hall KD**, **Kravitz AV.** Increases in physical activity result in diminishing increments in daily energy expenditure in mice. *Curr Biol* 27: 423–430, 2017. doi:10.1016/j.cub.2016.12.009.
8. **Duivenvoorde LP**, **van Schothorst EM**, **Swarts HJ**, **Keijer J.** Assessment of metabolic flexibility of old and adult mice using three noninvasive, indirect calorimetry-based treatments. *J Gerontol A Biol Sci Med Sci* 70: 282–293, 2015. doi:10.1093/gerona/glu027.
9. **König C**, **Plank A-C**, **Kapp A**, **Timotius IK**, **von Hörsten S**, **Zimmermann K.** Thirty mouse strain survey of voluntary physical activity and energy expenditure: influence of strain, sex and day–night variation. *Front Neurosci* 14: 531, 2020. doi:10.3389/fnins.2020.00531.
10. **Keipert S**, **Kutschke M**, **Ost M**, **Schwarzmayr T**, **van Schothorst EM**, **Lamp D**, **Brachthäuser L**, **Hamp I**, **Mazibuko SE**, **Hartwig S**, **Lehr S**, **Graf E**, **Plettenburg O**, **Neff F**, **Tschöp MH**, **Jastroch M.** Long-term cold adaptation does not require FGF21 or UCP1. *Cell Metab* 26: 437–446.e5, 2017. doi:10.1016/j.cmet.2017.07.016.
11. **Dickinson ME**, **Flenniken AM**, **Ji X**, **Teboul L**, **Wong MD**, **White JK**, **et al.** High-throughput discovery of novel developmental phenotypes. *Nature* 537: 508–514, 2016 [Erratum in *Nature* 551: 398, 2017]. doi:10.1038/nature19356.
12. **Péronnet F**, **Massicotte D.** Table of nonprotein respiratory quotient: an update. *Can J Sport Sci* 16: 23–29, 1991.
13. **Ferrannini E.** The theoretical bases of indirect calorimetry: a review. *Metabolism* 37: 287–301, 1988. doi:10.1016/0026-0495(88)90110-2.
14. **Elia M**, **Livesey G.** Theory and validity of indirect calorimetry during net lipid synthesis. *Am J Clin Nutr* 47: 591–607, 1988. doi:10.1093/ajcn/47.4.591.
15. **Stringer W**, **Casaburi R**, **Wasserman K.** Acid-base regulation during exercise and recovery in humans. *J Appl Physiol (1985)* 72: 954–961, 1992. doi:10.1152/jappl.1992.72.3.954.
16. **Wasserman K**, **Beaver WL**, **Whipp BJ.** Gas exchange theory and the lactic acidosis (anaerobic) threshold. *Circulation* 81: II14–30, 1990.
17. **Lusk G.** Analysis of the oxidation of mixtures of carbohydrate and fat: a correction. *J Biol Chem* 59: 41–42, 1924.
18. **Lusk G.** *The Elements of the Science of Nutrition*. Philadelphia, PR: WB Saunders, 1928.
19. **Hoevenaars FP**, **Keijer J**, **Swarts HJ**, **Snaas-Alders S**, **Bekkenkamp-Grovenstein M**, **van Schothorst EM.** Effects of dietary history on energy metabolism and physiological parameters in C57BL/6J mice. *Exp Physiol* 98: 1053–1062, 2013. doi:10.1113/expphysiol.2012.069518.
20. **Mina AI**, **LeClair RA**, **LeClair KB**, **Cohen DE**, **Lantier L**, **Banks AS.** CalR: a web-based analysis tool for indirect calorimetry experiments. *Cell Metab* 28: 656–666.e1, 2018. doi:10.1016/j.cmet.2018.06.019.
21. **Bier DM.** Intrinsically difficult problems: the kinetics of body proteins and amino acids in man. *Diabetes Metab Rev* 5: 111–132, 1989. doi:10.1002/dmr.5610050203.
22. **Liu Z**, **Barrett EJ.** Human protein metabolism: its measurement and regulation. *Am J Physiol Endocrinol Metab* 283: E1105–E1112, 2002. doi:10.1152/ajpendo.00337.2002.
23. **Fouillet H**, **Bos C**, **Gaudichon C**, **Tomé D.** Approaches to quantifying protein metabolism in response to nutrient ingestion. *J Nutr* 132: 3208S–3218S, 2002. doi:10.1093/jn/131.10.3208S.
24. **Livesey G**, **Elia M.** Estimation of energy expenditure, net carbohydrate utilization, and net fat oxidation and synthesis by indirect calorimetry: evaluation of errors with special reference to the detailed composition of fuels. *Am J Clin Nutr* 47: 608–628, 1988 [Erratum in *Am J Clin Nutr* 50: 1475, 1989] doi:10.1093/ajcn/47.4.608.
25. **Wilkinson DJ.** Historical and contemporary stable isotope tracer approaches to studying mammalian protein metabolism. *Mass Spectrom Rev* 37: 57–80, 2018. doi:10.1002/mas.21507.
26. **Engelen MP**, **Ten Have GA**, **Thaden JJ**, **Deutz NE.** New advances in stable tracer methods to assess whole-body protein and amino acid metabolism. *Curr Opin Clin Nutr Metab Care* 22: 337–346, 2019. doi:10.1097/MCO.0000000000000583.
27. **Pannemans DL**, **Wagenmakers AJ**, **Westerterp KR**, **Schaafsma G**, **Halliday D.** The effect of an increase of protein intake on whole-body protein turnover in elderly women is tracer dependent. *J Nutr* 127: 1788–1794, 1997. doi:10.1093/jn/127.9.1788.
28. **Wolfe RR**, **Park S**, **Kim I-Y**, **Starck C**, **Marquis BJ**, **Ferrando AA**, **Moughan PJ.** Quantifying the contribution of dietary protein to whole body protein kinetics: examination of the intrinsically labeled proteins method. *Am J Physiol Endocrinol Metab* 317: E74–E84, 2019. doi:10.1152/ajpendo.00294.2018.
29. **Grassian DT.** The dietary behaviors of participants in UK-based meat reduction and vegan campaigns–a longitudinal, mixed-methods study. *Appetite* 154: 104788, 2020. doi:10.1016/j.appet.2020.104788.
30. **Alae-Carew C**, **Green R**, **Stewart C**, **Cook B**, **Dangour AD**, **Scheelbeek PF.** The role of plant-based alternative foods in sustainable and healthy food systems: consumption trends in the UK. *Sci Total Environ* 807: 151041, 2022. doi:10.1016/j.scitotenv.2021.151041.
31. **Mann N**, **Pirotta Y**, **O'Connell S**, **Li D**, **Kelly F**, **Sinclair A.** Fatty acid composition of habitual omnivore and vegetarian diets. *Lipids* 41: 637–646, 2006. doi:10.1007/s11745-006-5014-9.
32. **Body DR.** The lipid composition of adipose tissue. *Prog Lipid Res* 27: 39–60, 1988. doi:10.1016/0163-7827(88)90004-5.